OL Organic Letters

pubs.acs.org/OrgLett

Letter

Chemically Triggered Release of Singlet Oxygen from Bisphenalenyl Endoperoxides with a Brønsted Acid

Muhammad Imran and Mark S. Chen*

Cite This: *Org. Lett.* 2022, 24, 1947−1952

Read Online

ACCESS | Metrics & More | Article Recommendations | Supporting Information

ABSTRACT: Aromatic endoperoxides have emerged as intriguing stimulus-responsive materials for molecular oxygen (O_2) storage and delivery but are currently limited in their application because they require heat to trigger O_2 release. Here we present the first example of acid-triggered singlet oxygen ($^1O_2$) release that does not require external heating by treating bisphenalenyl endoperoxides (EPOs) with trifluoroacetic acid. Mechanistic studies reveal that diprotonation of EPOs leads to a >10-fold increase in cycloreversion rates by lowering the energy of activation (ΔE_a) by as much as 71.1 kJ mol^{-1}. Remarkably, acid-catalyzed $^1O_2$ release is even demonstrated at room temperature. Chemical trapping experiments indicate that reactive $^1O_2$ is present during acid-triggered release, which is promising for the development of these molecular materials for metal-free, on-demand $^1O_2$ delivery.

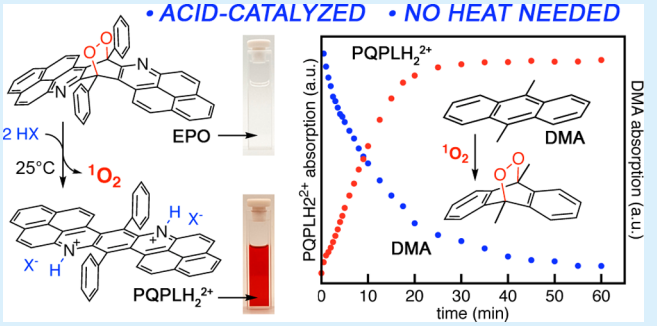

Aromatic compounds are attractive materials for sensing, storing, and delivering molecular oxygen (O_2) based on their ability to reversibly bind O_2.[1] Controlled release of O_2 in its reactive singlet form ($^1O_2$) is especially desirable from these materials because $^1O_2$ is useful for a wide variety of applications in chemical synthesis,[2,3] materials science,[4−7] and biology.[8−13]

The emergence of aromatic compounds as oxygen-responsive materials originates from their reversible reactivity with O_2 through the formation and decomposition of aromatic endoperoxides (Scheme 1).[14] Reactivity typically requires singlet oxygen ($^1O_2$) formation via photosensitization that undergoes a formal [4+2] cycloaddition with an arene to form an aromatic endoperoxide (EPO).[15−19] The release of oxygen from EPOs is activated by heating, to promote cycloreversion of the endoperoxide moiety and regenerate the parent arene via thermolysis.[20,21] Unfortunately, EPO cycloreversion often requires high temperatures (>80 °C), which limits their use under biologically relevant conditions. Some EPOs have demonstrated cycloreversion at room temperature, but their reliance on thermal activation requires that they be stored and handled at extremely low temperatures to prevent premature decomposition.[22,23] Therefore, for the purpose of discovering a metal-free material for $^1O_2$ delivery, it is critical to identify ambient-stable EPOs capable of chemically triggered O_2 release at or near room temperature.[24−28]

Prior to this study, there was only one example of metal-free, chemically triggered O_2 release, in which methylation and protonation were shown to enhance the rate of release of O_2 from dipyridylanthracene EPOs at increased temperatures.[29] However, O_2 release at room temperature was seen only with strong methylating agents (i.e., methyl trifluoromethanesulfonate or trimethyloxonium tetrafluoroborate), which the authors explained was due to steric destabilization upon

Scheme 1. (a) Reversible Reactivity of Arenes with Molecular Oxygen (O_2) to Form Aromatic Endoperoxides That Can Release O_2 via Thermolysis and (b) a Prior Example of Chemically Triggered O_2 Release Promoted by N-Methylation

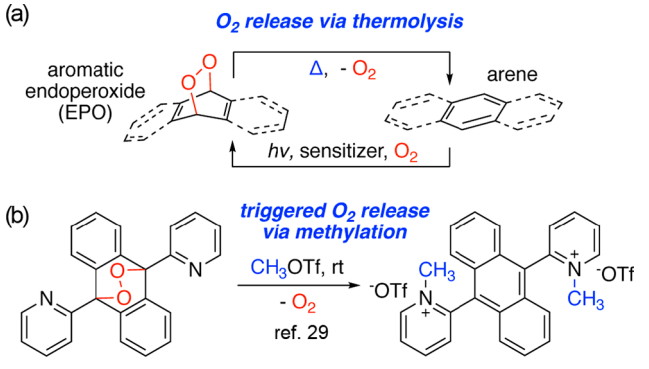

Received: January 30, 2022
Published: March 9, 2022

methylation (Scheme 1b). Because methylation and protonation of dipyridylanthracene EPOs both presumably generate dicationic species, we hypothesized that increasing the electrophilicity of EPOs via protonation of the N-functionality might facilitate cycloreversion, especially if that Lewis basic functionality is directly embedded in the π-backbone. Moreover, we surmised that protonation might be a simpler and more general activation mechanism because Brønsted acids versus methylating agents are tunable and likely to be compatible with a wider range of chemical environments.

Herein, we report the discovery of acid-triggered release of $^1O_2$ from bisphenalenyl EPOs upon their treatment with the simplest of chemical reagents: Brønsted acids. Kinetic measurements reveal that diprotonation is essential for acid-catalyzed cycloreversion by lowering ΔE_a and promoting >10-fold increases in rate. Chemical trapping experiments confirm that $^1O_2$ generation coincides with EPO cycloreversion, even at room temperature. Through these studies, we demonstrate the first example of acid-triggered release of $^1O_2$ from EPOs at room temperature.

We recently reported that bisphenalenyls **1**−**3** (PQPLs) are readily converted into ambient-stable EPOs (**1-O$_2$**−**3-O$_2$**) through self-sensitized reactivity with O_2 (Scheme 2).[30] This

Scheme 2. Interconversion of PQPLs and EPOs by Reactivity with Molecular Oxygen (O_2) and Our Proposed Mechanism for Acid-Triggered O_2 Release

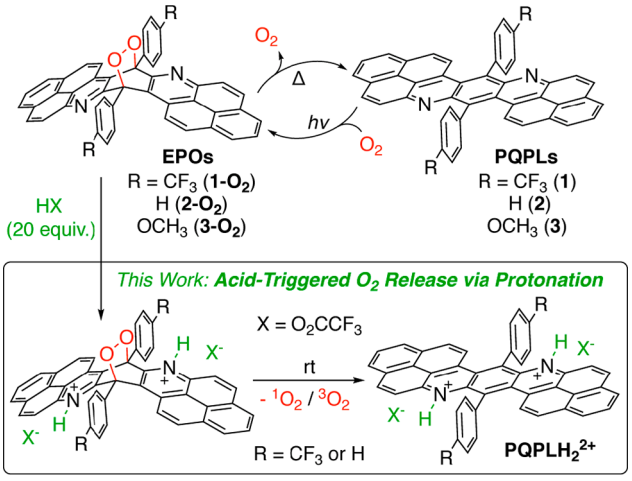

transformation coincides with a change in chromaticity from red to colorless that enables the use of PQPLs in colorimetric oxygen-sensing films. Because heating rapidly converts EPOs into their parent PQPL (**1**−**3**) through the release of O_2, EPO formation is reversible. Both binding and release of O_2 are very efficient, and minimal photochromic fatigue is observed even after multiple cycles. Encouraged by these results, we turned our focus to promoting EPO cycloreversions without the need for external heating. In particular, we were attracted to the potential of using acids to protonate our EPOs to generate more reactive species because they possess a Lewis basic N-functionality like dipyridylanthracene EPOs.[29] However, unlike dipyridylanthracene EPOs that possess pyridyl groups only appended to the π-backbone, our EPOs have pyridyl moieties fused into the π-backbone. Given that directly protonating the π-backbone versus induction from appended pyridinium groups is anticipated to have a stronger electronic effect, we postulated that electrophilic agents as simple as a proton (H^+) might promote cycloreversion in bisphenalenyl EPOs at substantially lower temperatures.

To explore the efficacy of acids for triggering cycloreversion, we treated dichloroethane solutions of EPOs (**1-O$_2$**−**3-O$_2$**) at 60 °C with a variety of Brønsted acids. Because O_2 release is expected to restore full conjugation in the π-backbone, we monitored reaction progress by looking for the rise of new absorption peaks above 500 nm. With weak acetic acid, even with a large stoichiometric excess (20 equiv), cycloreversion was sluggish and red-shifted features barely rose above the baseline even after 12 h (Figure S1). However, in the presence of excess (20 equiv) trifluoroacetic acid (TFA), cycloreversion proceeded at visibly higher rates where strong absorption features (~495, ~545, and ~585 nm) appeared within 1 h (Figure 1a,b). Attempts to decrease the number of equivalents of TFA led to sluggish reactivity (Figure S2), where new absorption peaks were even less prominent than in the case of

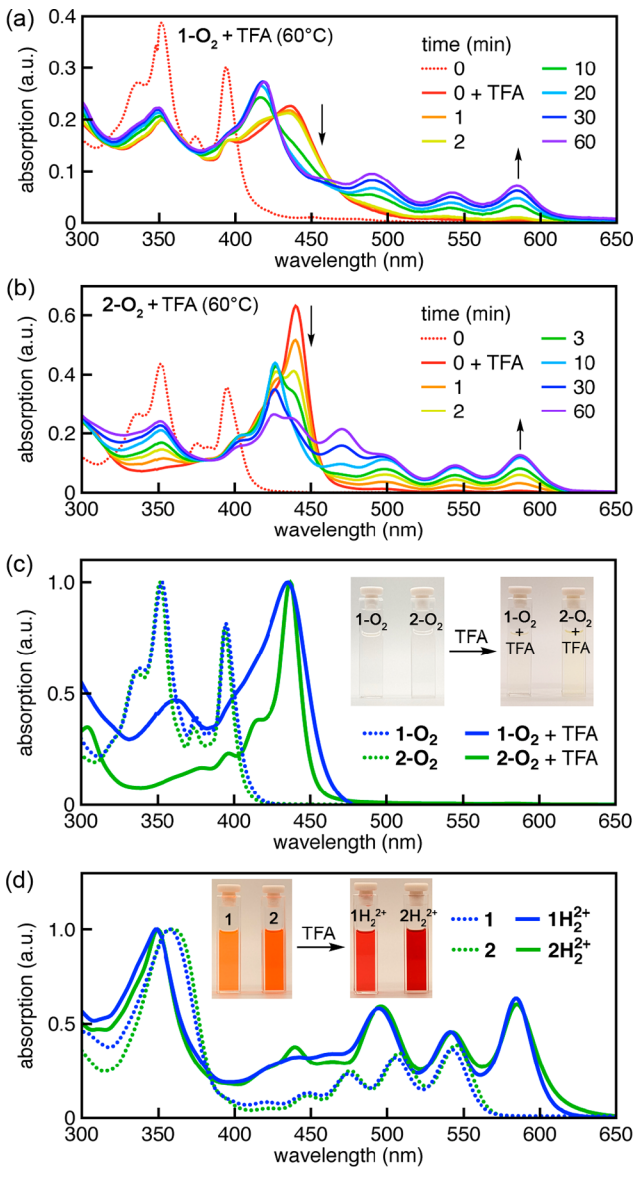

Figure 1. Plots of the change in absorption vs time for acid-triggered cycloreversion of (a) **1-O$_2$** and (b) **2-O$_2$** at 60 °C. Steady-state absorption spectra and photographs of solutions display the effects of adding TFA to (c) EPOs and (d) PQPLs.

https://doi.org/10.1021/acs.orglett.2c00340
Org. Lett. 2022, 24, 1947−1952

excess AcOH. The final products of acid-promoted cycloreversion are noticeably not PQPLs (**1** and **2**) but are instead diprotonated bisphenalenyls ($PQPLH_2^{2+}$, $\mathbf{1H_2}^{2+}$ and $\mathbf{2H_2}^{2+}$). The structure was confirmed by comparison with authentic samples synthesized independently from **1** and **2** via the addition of 20 equiv of CF_3CO_2D. Bisphenalenyls in this diprotonated form ($\mathbf{1H_2}^{2+}$ and $\mathbf{2H_2}^{2+}$) are inert to molecular oxygen and unable to generate aromatic endoperoxides, even in the presence of an external photosensitizer (Figure S3).

In contrast to $\mathbf{1\text{-}O_2}$ and $\mathbf{2\text{-}O_2}$, treatment of $\mathbf{3\text{-}O_2}$ with TFA led to the formation of only unidentifiable oxidized analogues of **3**. Because a stoichiometric excess of a strong acid is required to generate $PQPLH_2^{2+}$, this suggests that protonation of both pyridyls is necessary for promoting cycloreversion. An alternative decomposition pathway likely occurs in more electron-rich $\mathbf{3\text{-}O_2}$ because the endoperoxide moiety competes with the pyridyls for protonation. Consequently, protonation of the endoperoxide in $\mathbf{3\text{-}O_2}$ can promote cleavage of the O−O bond instead of the desired C−O bonds required for O_2 release.[22] Therefore, even though bisphenalenyl endoperoxides demonstrate acid-triggered O_2 release, strong electron-donating groups should be avoided in the molecular design to minimize the detrimental effects of endoperoxide basicity.

Spectroscopic characterization shows that the addition of TFA has a pronounced effect on the electronic structures of EPOs and PQPLs. Solutions of $\mathbf{1\text{-}O_2}$ and $\mathbf{2\text{-}O_2}$ that are normally colorless develop a yellow hue in the presence of TFA, due to a 50 nm absorption red-shift to ∼440 nm (Figure 1c). This red-shift is nearly identical to what is observed in spectra obtained when **1** and **2** are mixed with TFA to provide $\mathbf{1H_2}^{2+}$ and $\mathbf{2H_2}^{2+}$, respectively (Figure 1d). These similarities in spectral shifts between EPOs and PQPLs suggest that TFA leads to diprotonation of $\mathbf{1\text{-}O_2}$ and $\mathbf{2\text{-}O_2}$. ^{1}H NMR analysis of $\mathbf{2\text{-}O_2}$ upon addition of an excess (20 equiv) of TFA confirms that the initial species formed (∼440 nm peak) is diprotonated because the number of resonance peaks agrees with a symmetric (diprotonated) versus dissymmetric (monoprotonated) structure (Figure S6). Consequently, these data strongly suggest that diprotonation of $\mathbf{1\text{-}O_2}$ and $\mathbf{2\text{-}O_2}$ is necessary to promote EPO cycloreversion.

Titration of $\mathbf{2\text{-}O_2}$ with TFA provides further insight into the reaction course by allowing us to assign monoprotonation to the ∼420 nm peak (Figure S4). This peak is observed under less acidic conditions (Figures S1 and S2) but also appears to form in reactions with excess TFA as cycloreversion proceeds (Figure 1a,b), which suggests that acidity decreases with the release of more O_2. We postulate that this basification is due to dissolved O_2 quenching some of the TFA.[31] As the acidity of the reaction decreases, the equilibrium favors mono- versus diprotonated EPO. This inverse effect of O_2 concentration on acidity was confirmed by inducing an absorption blue-shift in a $\mathbf{2\text{-}O_2}$ solution treated with excess TFA (20 equiv) by simply bubbling O_2 for several minutes (Figure S5). The absorption blue-shift was then reversed by adding an additional 10 equiv of TFA. Altogether, these experiments strongly indicate that solution acidity is strongly affected by the concentration of solubilized O_2.

Because many applications for on-demand delivery require that O_2 be in its reactive singlet form ($^1O_2$), we monitored the acid-triggered cycloreversion of $\mathbf{2\text{-}O_2}$ in the presence of $^1O_2$ chemical traps. For qualitative analysis, we chose 9,10-dimethylanthracene (DMA) because it is relatively inert except for its known reactivity with $^1O_2$ to form an endoperoxide (DMA-O_2).[23,29] To ensure reactivity between DMA and any generated $^1O_2$, dichloroethane solutions of EPO ($\mathbf{2\text{-}O_2}$) and DMA were made in a 1:10 molar ratio (excess of the trap). Conversion of DMA was monitored by measuring the absorption at an isosbestic point (385 nm) in the conversion of $\mathbf{2\text{-}O_2}$ into $\mathbf{2H_2}^{2+}$, to ensure that changes in concentration were not convoluted by the presence of other species. Adding TFA immediately caused a decrease in the intensity of the peaks corresponding to DMA, and the growth of longer wavelength peaks representative of $\mathbf{2H_2}^{2+}$ (Figure 2a). Plotting

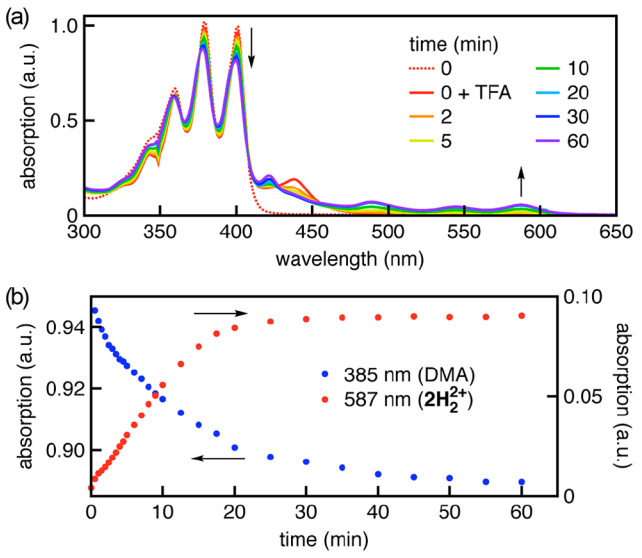

Figure 2. Singlet oxygen ($^1O_2$) trapping experiments that plot (a) the change in absorption vs time and (b) the time course of representative absorptions when $\mathbf{2\text{-}O_2}$ is treated with TFA (20 equiv) in the presence of 1,9-dimethylanthracene (DMA, 10 equiv) at 60 °C.

these absorption peaks versus time reveals a correlation between the conversion of DMA and the formation of $\mathbf{2H_2}^{2+}$ that strongly suggests that $^1O_2$ generated by EPO cycloreversion is subsequently trapped by reaction with DMA (Figure 2b). The results of trapping experiments with 1,3-diphenylbenzofuran (DPBF) were identical and also confirmed that $^1O_2$ is generated by acid-triggered EPO cycloreversion (Figures S8 and S9). For quantitative $^1O_2$ trapping, we performed acid-triggered O_2 release in the presence of excess (10 equiv) tetramethylethylene that is converted to a hydroperoxide (3-hydroperoxy-2,3-dimethylbut-1-ene) upon reaction with $^1O_2$. After 24 h at 60 °C, we measured a 39.4% yield for hydroperoxide formation by ^{1}H NMR analysis, which supports that at least 39% of the O_2 released is in its reactive singlet state (Figure S12).

To compare acid-promoted cycloreversion rates with those obtained under our previously reported, acid-free conditions, kinetic measurements were performed at 100 °C. Due to the higher temperature, we monitored solutions of EPOs in chlorobenzene versus dichloroethane. High reaction rates prevented whole spectra from being collected on such short time scales, so reaction progress was instead monitored by the rise of a representative peak for each $PQPLH_2^{2+}$: 580 nm for $\mathbf{1\text{-}O_2}$ and 585 nm for $\mathbf{2\text{-}O_2}$ (Figure 3). Cycloreversion follows first-order kinetics that correspond to half-lives of 60.0 ± 1.0 and 41.1 ± 1.5 s for $\mathbf{1\text{-}O_2}$ and $\mathbf{2\text{-}O_2}$, respectively. Although

https://doi.org/10.1021/acs.orglett.2c00340
Org. Lett. 2022, 24, 1947−1952

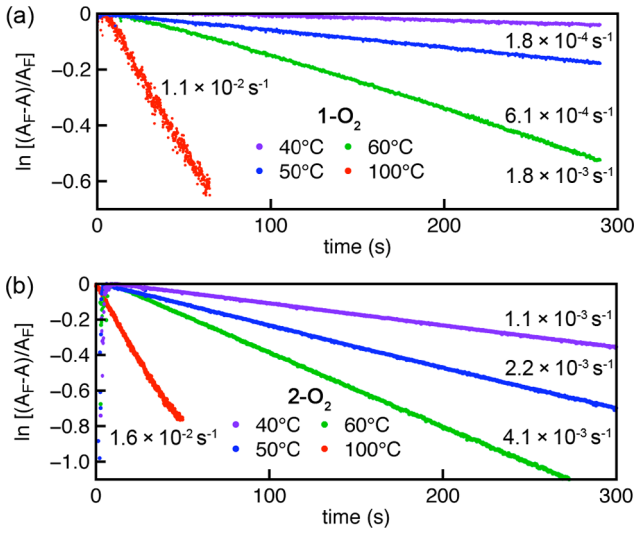

Figure 3. Logarithmic plots of the change in absorption vs time for acid-triggered EPO cycloreversion at 40−100 °C for (a) **1-O$_2$** and (b) **2-O$_2$**.

similar, the cycloreversion rate for **2-O$_2$** versus **1-O$_2$** is slightly higher, which reverses the trend observed under acid-free conditions where EPO electron deficiency trends with higher reactivity. This trend reversal likely results from the increased basicity of **2-O$_2$** versus **1-O$_2$**, which increases the formation of reactive diprotonated EPO species in solution. Additionally, compared to the kinetics of our acid-free reaction conditions, these data show that the addition of acid promotes a >10-fold increase in the rate of O_2 release. Given this strong effect, we sought to probe how diprotonation might affect the cycloreversion transition state.

Thermodynamic parameters of the transition state were determined from reaction kinetic measurements of acid-triggered EPO cycloreversion performed at different temperatures. Measurements were taken in dichloroethane solutions at identical EPO concentrations at three different temperatures: 40, 50, and 60 °C (Figure 3). Arrhenius plots reveal ΔE_a values of 96.4 and 52.9 kJ mol^{-1} for **1-O$_2$** and **2-O$_2$**, respectively (Table 1 and Figure S7). Both of these values are significantly lower than the ΔE_a values (115 kJ mol^{-1} for **1-O$_2$** and 124 kJ mol^{-1} for **2-O$_2$**) measured under acid-free conditions and confirm that acid has a catalytic effect on cycloreversion. Eyring analyses reveal that acid also causes a significant decrease in $\Delta H^{\ddagger}$, which is the major factor in lowering the ΔE_a for EPO cycloreversion (Figure S7). We postulate that increased electrophilicity in the π-backbone due to diprotonation leads to weakening of the C−O bonds, thereby facilitating O_2 release. For both EPOs, a decrease in transition-state entropy ($\Delta S^{\ddagger}$) is also observed when cycloreversion is promoted by acid. For **1-O$_2$**, the entropy decreases from −1.28 J K^{-1} mol^{-1} in the absence of acid to −17.7 J K^{-1} mol^{-1} with TFA. For **2-O$_2$**, the decrease in entropy is even greater as $\Delta S^{\ddagger}$ = −121 J K^{-1} mol^{-1} with TFA versus 20.3 J K^{-1} mol^{-1} in the absence of acid. These data suggest that the transition state is more conformationally restricted and agree with protonation of the pyridyl moieties creating greater steric hindrance to unbending of the EPO π-backbone.

The catalytic effect of diprotonation on EPO cycloreversion is powerful as we even observe acid-triggered O_2 release at room temperature (25 °C). At such a temperature, in the absence of acid, **2-O$_2$** is persistent and shows no changes to its absorption spectrum even after several months. However, when TFA is added, cycloreversion of **2-O$_2$** proceeds at a rate (k = 6.7 × 10^{-4} s^{-1}) akin to that of uncatalyzed thermolysis at elevated temperatures (Figure 4a,b). This result is only the second example of chemically triggered O_2 release at room temperature and is the first to be promoted by a simple Brønsted acid (TFA). Trapping experiments with DMA at 25 °C also confirm that $^1O_2$ is generated at this relatively low reaction temperature (Figure 4c and Figure S10).

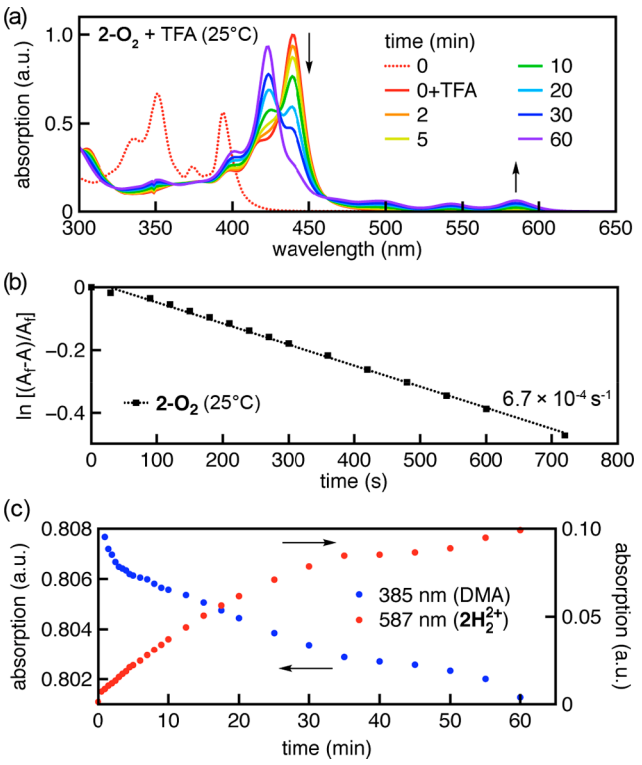

Figure 4. (a) Plot of the change in absorption vs time and (b) logarithmic plot of acid-triggered (20 equiv of TFA) cycloreversion of **2-O$_2$** at 25 °C. (c) Plot of representative absorptions vs time when acid-triggered cycloreversion of **2-O$_2$** is performed in the presence of 1,9-dimethylanthracene (DMA, 10 equiv).

Altogether, these examples of Brønsted acid-promoted reactivity at mild temperatures are very promising for the potential of EPOs to serve as all-organic, stimulus-responsive

Table 1. Kinetic and Thermodynamic Parameters of Cycloreversion of EPOs 1-O$_2$ and 2-O$_2$ in the Presence of an Acid (TFA, 20 equiv)

EPO	$t^{1/2}$ (s)[a]	k (×10^{-4} s^{-1})[a]	ΔE_a (kJ mol^{-1})	ln A	$\Delta H^{\ddagger}$ (kJ mol^{-1})	$\Delta S^{\ddagger}$ (J K^{-1} mol^{-1})
1-O$_2$	60.0 ± 1.0	107 ± 1.3	96.4 ± 0.2	28.5 ± 0.2	93.7 ± 0.2	−17.7 ± 0.6
2-O$_2$	41.1 ± 1.5	167 ± 7.8	52.9 ± 0.3	16.0 ± 0.1	50.2 ± 0.3	−121 ± 0.8

[a]Measured at 373 K in chlorobenzene.

https://doi.org/10.1021/acs.orglett.2c00340
Org. Lett. 2022, 24, 1947−1952

$^1O_2$ delivery materials. Given that acid−base reactivity is so well-understood, acid-responsive materials are certain to find many chemical and biological applications.[32] Ongoing investigations are focused on tuning these molecules so that O_2 release can be triggered under less acidic and even aqueous conditions.

■ ASSOCIATED CONTENT

Supporting Information

The Supporting Information is available free of charge at https://pubs.acs.org/doi/10.1021/acs.orglett.2c00340.

General synthetic methods, synthetic procedures and characterization, absorption spectroscopy, reaction kinetic measurements, singlet oxygen trapping experiments, references, and NMR spectra (PDF)

■ AUTHOR INFORMATION

Corresponding Author

Mark S. Chen − *Department of Chemistry, Lehigh University, Bethlehem, Pennsylvania 18015-3102, United States;* orcid.org/0000-0001-5415-4660; Email: mschen@lehigh.edu

Author

Muhammad Imran − *Department of Chemistry, Lehigh University, Bethlehem, Pennsylvania 18015-3102, United States;* orcid.org/0000-0002-9985-3542

Complete contact information is available at: https://pubs.acs.org/10.1021/acs.orglett.2c00340

Notes

The authors declare no competing financial interest.

■ ACKNOWLEDGMENTS

Acknowledgement is made to the Donors of the American Chemical Society Petroleum Research Fund for partial support of this research (61890-ND4). Support was also provided by a National Science Foundation (NSF) CAREER award (CHE-2045920) and Lehigh University. M.I. thanks the Fulbright Program for a Predoctoral Graduate Fellowship. This work made use of the Lehigh University NMR Facility and a Bruker Neo 500 MHz NMR instrument that was acquired through NSF Grant MRI-1725883, with additional support from Lehigh University.

■ REFERENCES

(1) Brega, V.; Yan, Y.; Thomas, S. W. Acenes Beyond Organic Electronics: Sensing of Singlet Oxygen and Stimuli-Responsive Materials. *Org. Biomol. Chem.* **2020**, *18*, 9191−9209.

(2) Ghogare, A. A.; Greer, A. Using Singlet Oxygen to Synthesize Natural Products and Drugs. *Chem. Rev.* **2016**, *116*, 9994−10034.

(3) Greer, A. Christopher Foote's Discovery of the Role of Singlet Oxygen [$^1O_2$ ($^1\Delta_g$)] in Photosensitized Oxidation Reactions. *Acc. Chem. Res.* **2006**, *39*, 797−804.

(4) He, Y.-Q.; Fudickar, W.; Tang, J.-H.; Wang, H.; Li, X.; Han, J.; Wang, Z.; Liu, M.; Zhong, Y.-W.; Linker, T.; Stang, P. J. Capture and Release of Singlet Oxygen in Coordination-Driven Self-Assembled Organoplatinum (II) Metallacycles. *J. Am. Chem. Soc.* **2020**, *142*, 2601−2608.

(5) Filatov, M. A.; Senge, M. O. Molecular Devices based on Reversible Singlet Oxygen Binding in Optical and Photomedical Applications. *Mol. Syst. Des. Eng.* **2016**, *1*, 258−272.

(6) Zehm, D.; Fudickar, W.; Linker, T. Molecular Switches Flipped by Oxygen. *Angew. Chem., Int. Ed.* **2007**, *46*, 7689−7692.

(7) Fudickar, W.; Fery, A.; Linker, T. Reversible Light and Air-Driven Lithography by Singlet Oxygen. *J. Am. Chem. Soc.* **2005**, *127*, 9386−9387.

(8) Fudickar, W.; Roder, P.; Listek, M.; Hanack, K.; Linker, T. Pyridinium Alkynylanthracenes as Sensitizers for Photodynamic Therapy. *Photochem. Photobiol.* **2022**, *98*, 193.

(9) Liu, M.; Ucar, E.; Liu, Z.; Wang, L.; Yang, L.; Xu, J.; Akkaya, E. U. Anticoagulant Activity of Singlet Oxygen Released from a Water Soluble Endoperoxide by Thermal Cycloreversion. *RSC Adv.* **2021**, *11*, 14513−14516.

(10) Wang, X.; Bittner, T.; Milanov, M.; Kaul, L.; Mundinger, S.; Koch, H.-G.; Jessen-Trefzer, C.; Jessen, H. J. Pyridinium Modified Anthracenes and Their Endoperoxides Provide a Tunable Scaffold with Activity against Gram-Positive and Gram-Negative Bacteria. *ACS Infect. Dis.* **2021**, *7*, 2073−2080.

(11) Ogilby, P. R. Singlet Oxygen: There is Indeed Something New Under the Sun. *Chem. Soc. Rev.* **2010**, *39*, 3181−3209.

(12) DeRosa, M. C.; Crutchley, R. J. Photosensitized Singlet Oxygen and its Applications. *Coord. Chem. Rev.* **2002**, *233*−*234*, 351−371.

(13) Pierlot, C.; Aubry, J.-M.; Briviba, K.; Sies, H.; Di Mascio, P. [1] Naphthalene Endoperoxides as Generators of Singlet Oxygen in Biological Media. *Methods Enzymol.* **2000**, *319*, 3−20.

(14) Aubry, J. M.; Pierlot, C.; Rigaudy, J.; Schmidt, R. Reversible Binding of Oxygen to Aromatic Compounds. *Acc. Chem. Res.* **2003**, *36*, 668−675.

(15) Liu, K.; Lalancette, R. A.; Jäkle, F. Tuning the Structure and Electronic Properties of B-N Fused Dipyridylanthracene and Implications on the Self-Sensitized Reactivity with Singlet Oxygen. *J. Am. Chem. Soc.* **2019**, *141*, 7453−7462.

(16) Liu, K.; Lalancette, R. A.; Jäkle, F. B-N Lewis Pair Functionalization of Anthracene: Structural Dynamics, Optoelectronic Properties, and O_2 Sensitization. *J. Am. Chem. Soc.* **2017**, *139*, 18170−18173.

(17) Fudickar, W.; Linker, T. Why Triple Bonds Protect Acenes from Oxidation and Decomposition. *J. Am. Chem. Soc.* **2012**, *134*, 15071−15082.

(18) Fudickar, W.; Linker, T. Theoretical Insights into the Effect of Solvents on the [4 + 2] Cycloaddition of Singlet Oxygen to Substituted Anthracenes: A Change from a Stepwise Process to a Concerted Process. *J. Phys. Org. Chem.* **2019**, *32*, e3951.

(19) Fudickar, W.; Linker, T. Remote Substituent Effects on the Photooxygenation of 9,10-Diarylanthracenes: Strong Evidence for Polar Intermediates. *Chem. Commun.* **2008**, 1771−1773.

(20) Turro, N. J.; Chow, M.-F.; Rigaudy, J. Mechanism of Thermolysis of Endoperoxides of Aromatic Compounds. Activation Parameters, Magnetic Field, and Magnetic Isotope Effects. *J. Am. Chem. Soc.* **1981**, *103*, 7218−7224.

(21) Turro, N. J.; Chow, M.-F.; Rigaudy, J. Thermolysis of Anthracene Endoperoxides. Concerted vs. Diradical Mechanisms. Microscopic Reversibility in Endothermic Chemiluminescent Reactions. *J. Am. Chem. Soc.* **1979**, *101*, 1300−1302.

(22) Bauch, M.; Krtitschka, A.; Linker, T. Photooxygenation of Oxygen-substituted Naphthalenes. *J. Phys. Org. Chem.* **2017**, *30*, e3734.

(23) Fudickar, W.; Linker, T. Release of Singlet Oxygen from Organic Peroxides under Mild Conditions. *ChemPhotoChem.* **2018**, *2*, 548−558.

(24) Lv, W.; Xia, H.; Zhang, K. Y.; Chen, Z.; Liu, S.; Huang, W.; Zhao, Q. Photothermal-Triggered Release of Singlet Oxygen from an Endoperoxide-Containing Polymeric Carrier for Killing Cancer Cells. *Mater. Horiz.* **2017**, *4*, 1185−1189.

(25) Kolemen, S.; Ozdemir, T.; Lee, D.; Kim, G. M.; Karatas, T.; Yoon, J.; Akkaya, E. U. Remote-Controlled Release of Singlet Oxygen by the Plasmonic Heating of Endoperoxide-Modified Gold Nanorods: Towards a Paradigm Change in Photodynamic Therapy. *Angew. Chem., Int. Ed.* **2016**, *55*, 3606−3610.

(26) Asadirad, A. M.; Erno, Z.; Branda, N. R. Photothermal Release of Singlet Oxygen from Gold Nanoparticles. *Chem. Commun.* **2013**, *49*, 5639−5641.
(27) Ghorai, P.; Dussault, P. H. A New Peroxide Fragmentation: Efficient Chemical Generation of $^1O_2$ in Organic Media. *Org. Lett.* **2009**, *11*, 4572−4575.
(28) Ghorai, P.; Dussault, P. H. Mild and Efficient Re(VII)-Catalyzed Synthesis of 1,1-Dihydroperoxides. *Org. Lett.* **2008**, *10*, 4577−4579.
(29) Fudickar, W.; Linker, T. Release of Singlet Oxygen from Aromatic Endoperoxides by Chemical Triggers. *Angew. Chem., Int. Ed.* **2018**, *57*, 12971−12975.
(30) Imran, M.; Chen, M. S. Self-Sensitized and Reversible O2 Reactivity with Bisphenalenyls for Simple, Tunable, and Multicycle Colorimetric Oxygen-Sensing Films. *ACS Appl. Mater. Interfaces* **2022**, *14*, 1817−1825.
(31) Vishnetskaya, M. V.; Vasin, A. V.; Solkan, V. N.; Zhidomirov, G. M.; Mel'nikov, M. Y. Activation of Molecular Oxygen in Trifluoroacetic Acid. *Russ. J. Phys. Chem. B* **2010**, *84*, 1905−1907.
(32) Bachelder, E. M.; Beaudette, T. T.; Broaders, K. E.; Dashe, J.; Fréchet, J. M. J. Acetal-Derivatived Dextran: An Acid-Responsive Biodegradable Material for Therapeutic Applications. *J. Am. Chem. Soc.* **2008**, *130*, 10494−10495.

https://doi.org/10.1021/acs.orglett.2c00340
Org. Lett. 2022, 24, 1947−1952